ISBN: 978-3-95450-191-5 doi:10.18429/JACoW-SRF2017-MOPB053

RF ENERGY HARVESTING OF HOM POWER *

Chen Xu[1], Ilan Ben-Zvi[1,2], Tianmu Xin[1], Qiong Wu[1]
[1] Brookhaven National Laboratory, Upton, New York 11973-5000, USA
[2] Stony Brook University, Stony Brook, New York 11794, USA

Abstract

In an accelerator cavity, Higher Order Modes (HOM) are generated by the current of the beam. The HOM power can reach tens of kilowatts per cavity in a high current accelerator, depending on the details of the beam and cavity design. In this report, we propose a novel RF harvesting system to convert the HOM power into DC power. The removal of this DC power from the cryogenic system is very efficient, and furthermore it may be used for various purposes such as driving RF amplifiers, charge batteries etc. We show that the efficiency of the harvesting system is very high. The proposed HOM power recycling system contains a multiple band harmonic RF coupler, broadband RF antenna system, a high power rectifier diode circuit and a DC load.

INTRODUCTION

High current linear accelerators (linacs) are becoming common. The higher the current, the higher is the HOMs' power. The HOM power spectrum is concentrated at harmonics of the bunch repetition frequency. When the accelerator operates as an Energy Recovery Linac (ERL), the required fundamental power required to operate the cavities is relatively very low. Yet, the HOM power can account for a significant fraction of the input RF power. In the ERL, the HOM power spectrum peaks at even harmonics of the bunch repetition frequency [1]. We propose an antenna system beaming the HOM RF power in a highly collimated pattern, followed by collection and conversion the RF power into DC power by arrays of diodes. A schematic HOM power collection and harvesting system is shown in Figure 1.

As a specific example, we will design a power removal and recycling system using a dual band RF horn antenna system and matched diode collection for a particular example of an ERL operating at 650 MHz.

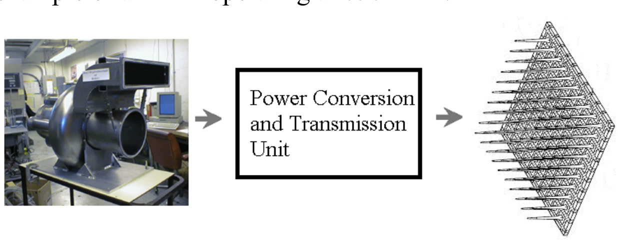

Figure 1: Schematic of an HOM power collection and conversion system. A CESR style cavity represents the HOM source on the left, a mode-converter and horn antenna is in the center and a diode array on the right.

This work is supported by Brookhaven Science Associates, LLC under Contract No. DE-AC02-98CH10886 with the U.S. DOE.
#chenxu@bnl.gov

This specific system will be operating at two frequency ranges: 1.3 and 2.6 GHz. We will explain why these two frequencies in the later sections in detail.

THE TRANSMISSION SYSTEM

The most common HOM out-coupling in accelerating cavities is a rectangular waveguide in TE10 mode. The field pattern of TE10 and TE11 in a rectangular waveguide, and the TE20 and TE11 in a circular waveguide are shown in Figure 2. From this figure, it is easy to see that the TE10 mode in rectangular waveguide can be easily converted to a TE11 in a circular waveguide. In addition, the TE11 mode in rectangular waveguide can be converted to a TE21 in a circular waveguide. In the circular horn, the energy densities of the TE11 and TE21 modes are distributed differently: The power of the TE11 is concentrated mainly about the axis center, while the TE21 has a null in the center. With an additional propagation distance, the power from these modes (which have different frequencies) are redistributed differently. The far field patterns of those modes form a circle enclosed by a ring. All simulations in this study are conducted in CST. [2]

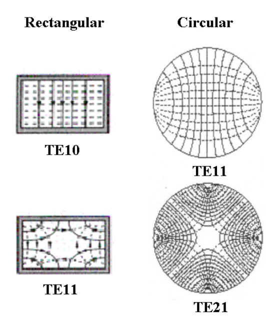

Figure 2: The field pattern of TE10 and TE10 in a rectangular waveguide, and the TE20 and TE11 in a circular waveguide.

To obtain a good directivity we use a conical horn antenna to launch the HOMs from a rectangular waveguide on a cavity. The far-fields of the horn antenna is the Fourier Transform of the fields at the opening of the horn. In addition, the radiation system is large enough for high power handling capacity, and experimental research is planned for the next step to study the ultimate power handling capacity. The HOM power generation in our example will be mostly at 1.3 and 2.6GHz, due to the ERL operation mode. We want to divide the 1.3GHz and 2.6GHz towards different destinations on the diode arrays, to optimize the harvesting unit energy conversion

ISBN: 978-3-95450-191-5 doi:10.18429/JACoW-SRF2017-MOPB053

efficiency. The two HOM bands originate as TE10 modes in the cavity's HOM waveguide port. In order to achieve the above-mentioned separation, we employ a mode converter between the HOM port and the horn antenna. The converter and horn design is depicted in Figure 3, and Table 1 provides a detailed list of the modes at the end of each element according to the mode's frequency.

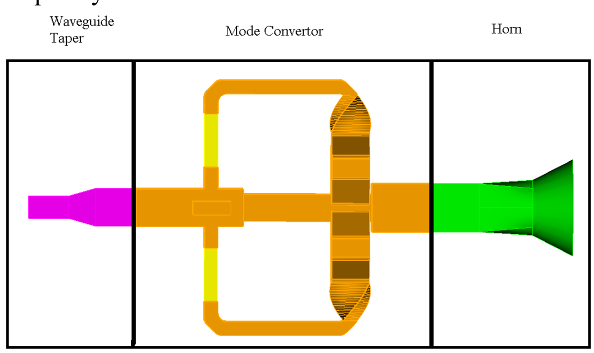

Figure 3: The final assembly of the transmission: The mode converter (orange) and horn (green).

Table1: The Modes at Two Frequencies at the End of the Various Sections (different color codes)

Frequency	Waveguide Taper	Mode converter	Horn
1.3GHz	TE10	TE11	TE21
2.6GHz	TE10	TE10	TE11

THE MODE CONVERTER

The mode converter unit connects the cavity to the horn radiator section. It is used to pass the TE10 mode at 2.6GHz, but convert the 1.3GHz TE10 HOM from the cavity to TE11 at its output. The converter begins as a tapered rectangular waveguide with a standard WR650 waveguide for input and a square section output. At the input (designated as port 1) to the WR650 wave port, the TE10 modes have two frequencies, 1.3GHz and 2.6GHz. The TE10 mode at 1.3GHz will be filtered out by the reduced square waveguide in Figure 4(~~seen~~ in the center of the mode converter in Figure 3), but it is split and propagated as TE10 in the side arms. The TE10 at 2.6GHz is propagated through the reduced dimension rectangular waveguide to the exit of the mode converter, designated as port 2. The 2.6 GHz is blocked from entering the side arms by low-pass filters [3], which are marked in yellow in Figure 3.

The transmission of the mode converter for the TE10 mode at 2.6GHz is -0.8db, with a reflection of -13db. Meanwhile at 1.3GHz, the reflection is -26db and insertion loss is -0.2db.

The conversion of the 1.3GHz TE10 mode to a TE11 mode proceeds as follows: The two arms propagate the TE10 mode in the H plane, and the short end stub with 90 degree of propagating arm in the E plane are used for matching condition for both frequencies.

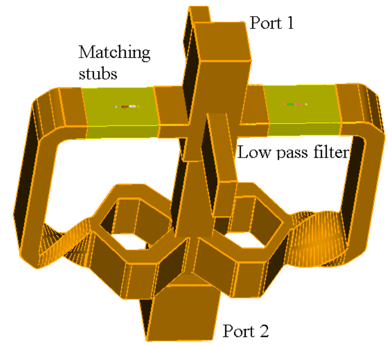

Figure 4: A view showing the design of mode divider and mode combiner. Port numbers are shown.

Next the two arms are twisted into the E plane and further separated into 4 arms, with TE10 modes in each of the four short waveguide. The four waveguides are fed into the square waveguide in the middle section to superimpose into the desired TE11 mode. The TE11 can propagate only towards the output (port 2) through the enlarged square waveguide, but not backwards to the input thanks to the smaller dimension of the square waveguide in that direction.

DESIGN OF THE HORN

Figure 5 illustrates the transition from the square waveguide to the conical horn via a polygonal section waveguide with twisted elements. In this section, the TE10 and TE11 modes in the input square wave port are converted into TE11 and TE21 modes in the circular waveguide and then radiated by the conical horn. The total reflections are less than -10dB for either mode.

The T11 and TE21 modes have different energy distributions in the circular: Most of the energy of the TE11 mode (at 2.6GHz) is near the axis, while the TE21 (at 1.3GHz) is distributed near the waveguide wall.

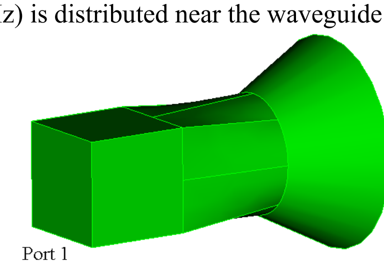

Figure 5: The design of the tapered waveguide and horn.

The far-field electromagnetic patterns of both modes have been simulated. The schematic illustration is shown in Figure 6. The E field pattern suggest that the TE11 energy is concentrated around the axis, while that of the TE21 vanishes on the axis is peaked around a cone emanating from the horn. The cone angle is related to the horn's opening angle and defines the placement of the energy harvesting arrays. Thus, this unit could transmit the RF power at the different frequencies to different zones.

ISBN: 978-3-95450-191-5 doi:10.18429/JACoW-SRF2017-MOPB053

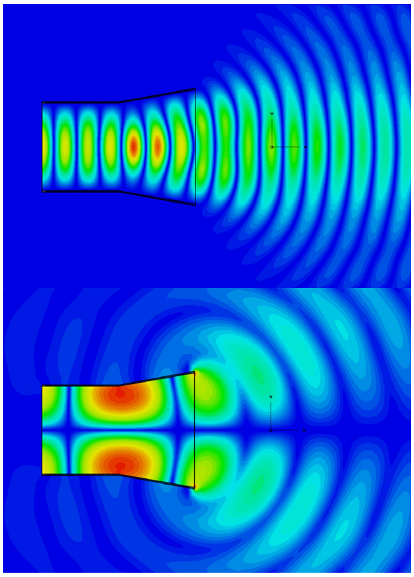

Figure 6: The field patterns of TE11(left)/TE21(right) in the horn and the possible curve short plane setup.

The RF rectification arrays are arranged on a curved plane, which conforms to the phase fronts of radiation fields of the two modes, leading to a field incident angle of 90° [4, 5] at the absorption plane. Thanks to the spatial separation of the modes at the rectification plane, selecting properly tuned diodes for each frequency enhances the efficiency of the system. The rectification planes, with 2 parabolic sections is shown in the Figure 7.

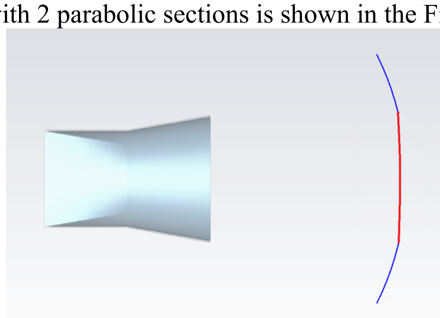

Figure 7: The cross sections of the energy collection surfaces is shown is shown in red for the TE11 mode and in blue for the TE21.

The field strength and power distribution of both modes is plotted as a function of the radius in Figure 8, demonstrating the mode separation.

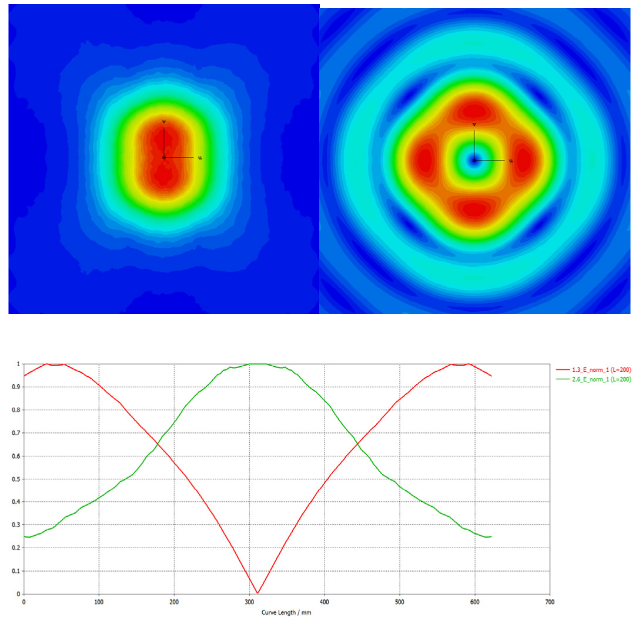

Figure 8: The E field patterns in the horn: TE11(upper left)/TE21(upper right) and the normalized energy density (lower) along the absorption planes.

SUMMARY

In this report, we propose a new scheme of handling waste power from HOM modes, beneficial for high-current linacs. The design converts dual band RF power to DC power with good conversion efficiency. This system reduces the cryogenic load of the removal of the HOM power from the cavities and makes it available for waste energy recovery. In this study, an example of a RF harvesting unit is shown at HOM frequencies of 1.3GHz and 2.6GHz. This example, while still not fully optimized, demonstrates a novel approach to the removal of high HOM power loads from superconducting cavities.

ACKNOWLEDGMENT

We would like to thank Haipeng Wang in Jefferson lab, and Sami Tantawi from SLAC for the useful discussions.

REFERENCES

[1] C. Xu, Nucl. Instr. and Meth. A. V 867, 21 (2017), pp 163–170.

[2] http://www.CST.com

[3] W. Schwab and W. Menzel, "Compact bandpass filters with improved stop-band characteristics using planar multilayer structures," in IEEE MTT-S Symp. Dig., 1992, pp. 1207–1210.

[4] S. Tantawi, Phys. Rev. Lett., 112 (2014), p. 164802.

[5] M. Straughn, C.-C. Chen, Proc. 10th European Conference on Antennas and Propagation (EuCAP), Davos, April, 2016.